

ISSN: 0256-307X

中国物理快报

Chinese Physics Letters

Volume 28 Number 4 April 2011

A Series Journal of the Chinese Physical Society
Distributed by IOP Publishing

Online: <http://iopscience.iop.org/cpl>
<http://cpl.iphy.ac.cn>

CHINESE PHYSICAL SOCIETY
Institute of **Physics** PUBLISHING

JOURNAL FOR AUTHORS
— CHINESE PHYSICS LETTERS

Sensitive Detection of Individual Neutral Atoms in a Strong Coupling Cavity QED System *

ZHANG Peng-Fei(张鹏飞)¹, ZHANG Yu-Chi(张玉驰)¹, LI Gang(李刚)¹, DU Jin-Jin(杜金锦)¹,
ZHANG Yan-Feng(张艳峰)¹, GUO Yan-Qiang(郭奕强)¹, WANG Jun-Min(王军民)¹,
ZHANG Tian-Cai(张天才)^{1**}, LI Wei-Dong(李卫东)²

¹State Key Laboratory of Quantum Optics and Quantum Optics Devices, Institute of Opto-Electronics, Shanxi University, Taiyuan 030006

²Department of Physics and Institute of Theoretical Physics, Shanxi University, Taiyuan 030006

(Received 6 January 2011)

We experimentally demonstrate real-time detection of individual cesium atoms by using a high-finesse optical micro-cavity in a strong coupling regime. A cloud of cesium atoms is trapped in a magneto-optical trap positioned at 5 mm above the micro-cavity center. The atoms fall down freely in gravitation after shutting off the magneto-optical trap and pass through the cavity. The cavity transmission is strongly affected by the atoms in the cavity, which enables the micro-cavity to sense the atoms individually. We detect the single atom transits either in the resonance or various detunings. The single atom vacuum-Rabi splitting is directly measured to be $\Omega = 2\pi \times 23.9$ MHz. The average duration of atom-cavity coupling of about 110 μ s is obtained according to the probability distribution of the atom transits.

PACS: 42.50.Pq, 37.10.Gh

DOI: 10.1088/0256-307X/28/4/044203

Sensitive detection of single atoms has always been a difficult task during the development of atomic physics.^[1] Fortunately, cavity quantum electrodynamics (CQED)^[2,3] in strong coupling regimes provide a powerful tool to detect single atoms sensitively. In the early period, Kimble *et al.*^[4,5] observed the atoms from a thermal atom beam by means of a high-finesse optical cavity. In the experiment the average atom number $N < 110$ was detected, however a deterministic single atom could not be observed due to the large velocities of thermal atoms. The durations of thermal atoms in the cavity are only several microseconds. This situation has changed until the naissance of the cold atom technology. In 1996, Mabuchi *et al.*^[6] investigated the real-time detection of individual atoms falling through a high-finesse optical Fabry-Perot cavity. Later, Hood *et al.*^[7] observed the single atoms passing through a cavity with various detunings and the “vacuum-Rabi” splitting was obtained. Other schemes such as optical fountain were also used to launch cold atoms into micro-cavities to reach the strong coupling between atoms and photons.^[8] Although in free space the substantial extinction of a light beam by a single atom was observed, which could be used to sense the single atom,^[9] the strongly coupled cavity QED can greatly enhance the ability of single atom sensing, not only for the sensitivity of a single atom^[7] but also for the spatial resolution.^[10] With the help of spatial symmetry breaking of the tilted high-order transverse cavity mode, the measurement

of spatial resolution of single atoms can be essentially improved.^[11] The detection of individual atoms can be used to investigate the statistical properties of the thermal atoms or an atom laser.^[12]

As an important and subtle system, cavity quantum electrodynamics in the strong coupling regime has greatly promoted the development of quantum optics and quantum information science^[13] during the past two decades. Besides the single atom detection, it has been used in diverse areas such as the generation of deterministic and controllable single-photon sources.^[14–16] Strongly coupled CQED has comprehensively improved the performance of single atom detection and quantum state control. By using the vacuum-stimulated Raman adiabatic passage (v-STIRAP), quantum states can be generated, such as the well-defined single photon state^[16] and quantum entangled state between atoms and photons.^[17] The strong coupling is also necessary to achieve the reversible mapping of quantum states between atoms and photons, which provides the basis for quantum optical interconnects and is a fundamental primitive for networks.^[18]

A common and effective method to achieve strong coupling is to reduce the effective mode volume of cavity. The optimal coupling coefficient g_0 between atoms and photons is $g_0 = d\sqrt{\hbar\omega/2\varepsilon_0V_m}$, where d is the atomic matrix element, ω the transition frequency, V_m the cavity mode volume. For a real system^[19] there are two decays, i.e. the atomic dipole decay rate γ

*Supported by the National Natural Science Foundation of China under Grant Nos 10794125, 60808006, 60821004, 61078051 and 60978017.

**Email: tczhang@sxu.edu.cn

© 2011 Chinese Physical Society and IOP Publishing Ltd

and the cavity decay rate κ . When the coupling coefficient g_0 is larger than the decay rates γ and κ , the strong coupling between atoms and cavity is achieved. The detuning between cavity and atom is described by $\Delta_{ca} = \omega_{\text{cavity}} - \omega_{\text{atom}}$ and the detuning between probe and atom is $\Delta_{pa} = \omega_{\text{probe}} - \omega_{\text{atom}}$. The cavity transmission in the weak-field limit of small excitation is

$$T(x, y) = \kappa^2 (\gamma^2 + \Delta_{pa}^2) \times \left\{ [g_{\text{eff}}(x, y)^2 - \Delta_{pa}^2 + \Delta_{ca} \Delta_{pa} + \gamma \kappa]^2 + (\kappa \Delta_{pa} + \gamma \Delta_{pa} - \gamma \Delta_{ca})^2 \right\}^{-1}, \quad (1)$$

where the effective coupling coefficient is $g_{\text{eff}}(x, y) = g_0 \Psi_{m,n}(x, y, z) / \Psi_{0,0}(0, 0)$. The mode functions read

$$\Psi_{m,n}(x, y) = C_{m,n} \exp\left(-\frac{x^2 + y^2}{w_0^2}\right) \times H_m\left(\frac{\sqrt{2}x}{w_0}\right) H_n\left(\frac{\sqrt{2}y}{w_0}\right), \quad (2)$$

where $C_{m,n} = (2^m 2^n m! n!)^{-1/2} (w_0^2 \pi / 2)^{-1/2}$ and $H_{m,n}$ are the corresponding Hermite polynomials of order m and n ; w_0 is the waist of the cavity mode; λ is the wavelength.

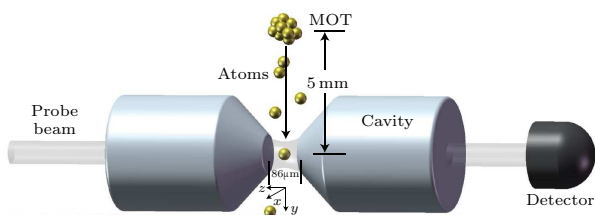


Fig. 1. (Color online) Schematic of the experimental setup. The length of the cavity is $86 \mu\text{m}$. The finesse of cavity is $F = 330000$ and the parameters of the system are $(g_0, \kappa, \gamma) = 2\pi \times (23.9, 2.6, 2.6)$ MHz. The MOT with about 10^5 atoms is positioned at 5 mm above the cavity. The atoms fall down and through the cavity mode after shutting off the MOT and the transmissions of the cavity are detected by the SPCMs.

In this study, we demonstrate the ultra-sensitive detection of individual cesium atoms passing through a high-finesse optical micro-cavity. The distinct result is that both the position and the velocity of the individual atoms are determined with high precision and a theoretical model is used to fit the experimental data. The micro-cavity is a Fabry-Perot cavity composed of two spherical mirrors with ultrahigh reflectivity and the length of the cavity is $86 \mu\text{m}$. The system is shown in Fig. 1. The MOT with about 10^5 atoms^[20–22] is located at 5 mm above the cavity. The waist of TEM₀₀ mode is $w_0 = 23.8 \mu\text{m}$. The finesse of cavity is $F = 330000$ and the parameters of the system are $(g_0, \kappa, \gamma) = 2\pi \times (23.9, 2.6, 2.6)$ MHz.^[23] The optimal coupling coefficient g_0 is much larger than the cavity decay rate κ and the atom decay rate γ , corresponding to the critical atom number

$N_0 = 2\kappa\gamma/g_0^2 = 0.024$ and critical photon number: $m_0 = \gamma^2/(2g_0^2) = 0.006$, so the CQED system reaches the strong coupling regime. The intra-cavity mean photon number is $m \approx 1$. The cavity transmission is detected by single photon counting modules (SPCMs, PerkinElmer).^[24,25] The probe light is adjusted to resonance with the cesium D2 ($6^2S_{1/2}, F = 4 \rightarrow 6^2P_{3/2}, F' = 5$) transition (wavelength is $\lambda = 852.36 \text{ nm}$).

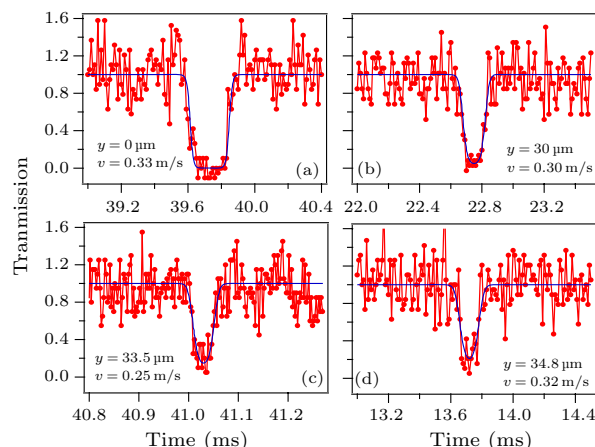


Fig. 2. The cavity transmissions versus time with atoms passing through the TEM₀₀ mode of cavity for $\Delta_{ca} = \Delta_{pa} = 0$. The intra-cavity mean photon number is $m \approx 1$. The atom is released at $t=0$ with shutting off the MOT. The position and the velocity of the atom for each transit are shown.

The coupling coefficient between the cavity TEM₀₀ mode and atom is dependent on the spatial position and can be described by the relation $g(\mathbf{r}) = g_0 \exp[-(x^2 + y^2)/w_0^2] \cos(2\pi z/\lambda)$, where x , y and z are the spatial coordinates shown in Fig. 1. It is found that the coupling coefficient can be changed from 0 (atom is at a node) to maximum (atom is at an antinode), depending on the location of the atom. When both the detunings are set to be $\Delta_{ca} = \Delta_{pa} = 0$, the empty cavity transmission keeps the maximum because of the resonance between the cavity and probe light. As the atom enters into the cavity, depending on its exact location, the cavity transmission will decrease since the strong coupling between the cavity and the atom causes the Rabi splitting and the probe beam will not be resonant to the cavity anymore. The cavity transmission will recover later to the maximum as the atom leaves the cavity. Figure 2 shows the typical four transits. The red dots and lines are experimental data and the blue solid curves are theoretical fitting according to Eq. (1). The process described above is clearly seen and the exact time when the atom arrives at the center of the cavity mode can be determined after it is released at $t = 0$. The experimental results show that the depth of each dip is different. From Fig. 2(a)–2(d), we can find that the coupling coefficients decrease. In Fig. 2(a) the transmission decreases to zero, which cor-

responds to $g_{\max}(\mathbf{r}) \approx g_0$ and implies that the atom almost flies through an antinode of the TEM_{00} mode, i.e., $y = 0$. From the depth of the dip, we can thus determine the position of the atom in the y direction. The shallower the dip is, the farther the atom is from the cavity axis. In Fig. 2(d), y is about $34.8 \mu\text{m}$, which is even larger than the radius of the mode waist. This means that even if the atom is far away from the cavity mode, it can still be detected sensitively. Actually, according to the theory, based on our system, even if the atom has $39 \mu\text{m}$ off-axis, 50% of the dip could still be observed. By measuring the transit time precisely, the velocity of the atom flying through the cavity can also be determined, as shown in Fig. 2.

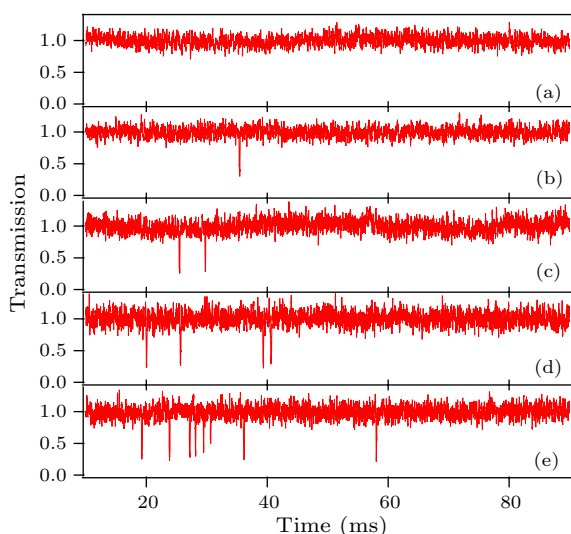


Fig. 3. The time-varying cavity transmissions with repetitive drops. There are 0, 1, 2, 4 and 8 atoms [(a)–(e)] flying through the cavity mode, respectively.

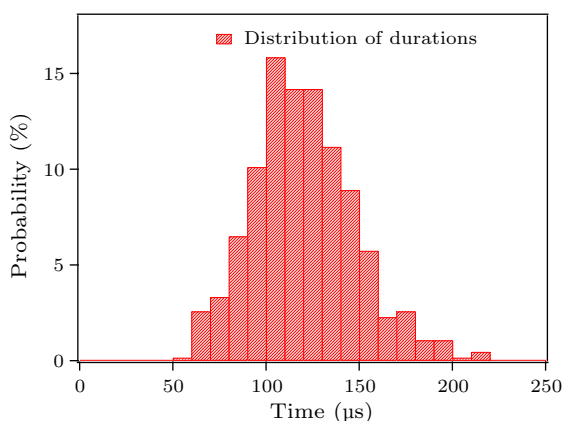


Fig. 4. Histogram of atom durations inside the cavity. The duration is obtained by the full width half maximum of the dips. The average atom duration is about $110 \mu\text{s}$.

We have measured the time-varying cavity transmission spectra with repetitive atom droppings, as shown in Fig. 3. Without atoms, the empty cavity transmission is shown in Fig. 3(a). From Figs. 3(b)–3(e), one can see 1, 2, 4 and 8 atoms flying through

the cavity mode, respectively. Single atoms can thus be counted one by one and the micro-cavity here acts just as a point-like single atom detector. From Fig. 3 we can see that the arrival times and the dip depths of the atom transits are stochastic. We can change the average atom number passing through the cavity mode every drop by adjusting the initial atom number of the atoms in the MOT and the falling status. There is an average of three atoms for every drop in our experiment. We have finished 220 drops and obtained a total of 664 atom transits. The histogram of atom transits is displayed in Fig. 4, which shows that the average single atom duration inside the cavity is about $110 \mu\text{s}$.

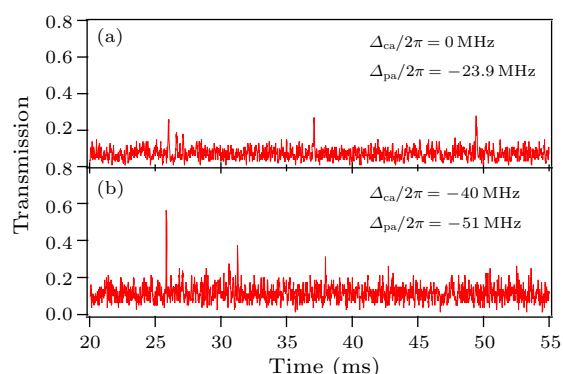


Fig. 5. The cavity transmission spectra with different probes and cavity detunings when the atom passes through the cavity mode. (a) $\Delta_{ca}/2\pi = 0$ and $\Delta_{pa}/2\pi = -23.9 \text{ MHz} = -g_0$, (b) $\Delta_{ca}/2\pi = -40 \text{ MHz}$ and $\Delta_{pa}/2\pi = -51 \text{ MHz}$.

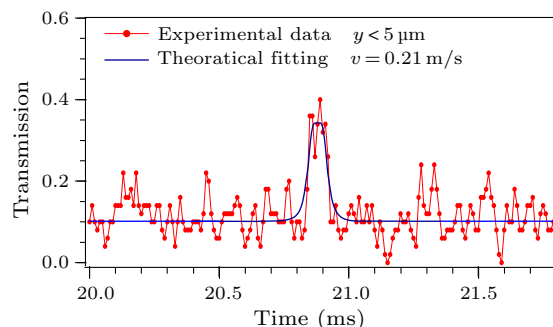


Fig. 6. The close look of the cavity transmission with the detunings $\Delta_{ca}/2\pi = 0$ and $\Delta_{pa}/2\pi = -23.9 \text{ MHz} = -g_0$. The red dots and line are the experimental results while the blue curve is the theoretical fitting according to the experimental parameters.

A single atom can also be detected in the case of non-resonance. We present the cavity transmission spectra with different detunings in Fig. 5. With $\Delta_{ca}/2\pi = 0$ and $\Delta_{pa}/2\pi = -23.9 \text{ MHz} = -g_0$, the cavity transmission keeps at low level when there is no atom in the cavity. As the atom flies through the cavity, we obtain a transmission peak, as shown in Fig. 5(a). Similar observation of the cavity transmission with the detuning of $\Delta_{ca}/2\pi = -40 \text{ MHz}$ and

$\Delta_{\text{pa}}/2\pi = -51$ MHz is shown in Fig. 5(b).

According to the experimental parameters, the maximum coupling coefficient is $g_0 = 2\pi \times 23.9$ MHz. Figure 6 is the close-up view of the cavity transmission for the detunings of $\Delta_{\text{ca}}/2\pi = 0$ and $\Delta_{\text{pa}}/2\pi = -23.9$ MHz. The peak in the center is the left peak due to the vacuum Rabi splitting, which can be seen clearly. The blue curve is the theoretical fitting according to our experimental parameters and the weak-field approximation. The experimental result agrees well with the theoretical simulation. Vacuum Rabi frequency $\Omega = 2g_0 = 2\pi \times 47.8$ MHz is thus confirmed directly.

In summary, we have experimentally investigated the sensitive measurement of individual neutral cesium atoms based on a strong coupling CQED system. The high-finesse optical micro-cavity can sense the single atom even if the atom is far away from the center of the cavity mode. The position and the velocity of the atom are both determined by the transmission spectra of the cavity. The average duration of the single atom in the cavity is about 110 μs . By setting the proper cavity and probe detunings, the transmission peak due to the vacuum Rabi splitting is observed directly, which confirms the strong coupling interaction and the vacuum Rabi frequency $\Omega = 2g_0 = 2\pi \times 47.8$ MHz. Such a strong coupling CQED system can be used for demonstrating the quantum manipulation and quantum measurement on the single quanta level.

References

- [1] Wang J, He J, Qiu Y, Yang B D, Zhao J Y, Zhang T C and Wang J M 2008 *Chin. Phys. B* **17** 2062
- [2] Berman P 1994 *Cavity Quantum Electrodynamics* (San Diego: Academic)
- [3] Zhang Y C, Li G, Zhang P F, Wang J M and Zhang T C 2009 *Front. Phys. Chin.* **4** 190
- [4] Rempe G, Thompson R J, Brecha R J, Lee W D and Kimble H J 1991 *Phys. Rev. Lett.* **67** 1727
- [5] Thompson R J, Rempe G and Kimble H J 1992 *Phys. Rev. Lett.* **68** 1132
- [6] Mabuchi H, Turchette Q A, Chapman M S and Kimble H J 1996 *Opt. Lett.* **21** 1393
- [7] Hood C J, Chapman M S, Lynn T W and Kimble H J 1998 *Phys. Rev. Lett.* **80** 4157
- [8] Munstermann P, Fischer T, Pinkse P W H and Rempe G 1999 *Opt. Commun.* **159** 63
- [9] Tey M K, Chen Z L, Aljunid S A, Chng B, Huber F, Maslennikov G and Kurtsiefer C 2008 *Nature Phys.* **4** 924
- [10] Hood C J, Lynn T W, Doherty A C, Parkins A S and Kimble H J 2000 *Science* **287** 1447
- [11] Zhang P F, Guo Y Q, Li Z H, Zhang Y F, Du J J, Li G, Wang J M and Zhang T C 2010 arXiv:1012.2156
- [12] Ottl A, Ritter S, Kohl M and Esslinger T 2005 *Phys. Rev. Lett.* **95** 090404
- [13] Monroe C 2002 *Nature* **416** 238
- [14] Kuhn A, Hennrich M and Rempe G 2002 *Phys. Rev. Lett.* **89** 067901
- [15] McKeever J, Boca A, Boozer A D, Miller R, Buck J R, Kuzmich A and Kimble H J 2004 *Science* **303** 1992
- [16] Hijlkema M, Weber B, Specht H P, Webster S C, Kuhn A and Rempe G 2007 *Nature Phys.* **3** 253
- [17] Volz J, Weber M, Schlenk D, Rosenfeld W, Vrana J, Saucke K, Kurtsiefer C and Weinfurter H 2006 *Phys. Rev. Lett.* **96** 030404
- [18] Kimble H J 2008 *Nature* **453** 1023
- [19] Carmichael H J 1993 *An Open Systems Approach to Quantum Optics* (Berlin: Springer)
- [20] Yan S B, Liu T, Geng T, Zhang T C, Peng K C and Wang J M 2004 *Chin. Phys.* **13** 1669
- [21] Geng T, Yan S B, Wang Y H, Yang H J, Zhang T C and Wang J M 2005 *Acta Phys. Sin.* **54** 5104 (in Chinese)
- [22] Zhang P F, Li G, Zhang Y C, Guo Y G, Wang J M and Zhang T C 2009 *Phys. Rev. A* **80** 053420
- [23] Li G, Zhang Y C, Li Y, Wang X Y, Zhang J, Wang J M and Zhang T C 2006 *Appl. Opt.* **45** 7628
- [24] Li G, Zhang T C, Li Y and Wang J M 2005 *Phys. Rev. A* **71** 023807
- [25] Li Y, Li G, Zhang Y C, Wang X Y, Zhang J, Wang J M and Zhang T C 2007 *Phys. Rev. A* **76** 013829

Chinese Physics Letters

Volume 28

Number 4

2011

GENERAL

- 040201 **A Field Integration Method for a Nonholonomic Mechanical System of Non-Chetaev's Type**
XIA Li-Li
- 040202 **A Modification of Extended Homoclinic Test Approach to Solve the (3+1)-Dimensional Potential-YTSF Equation**
M. T. Darvishi, Mohammad Najafi
- 040203 **Perturbation to Noether Symmetry and Noether adiabatic Invariants of Discrete Mechanico-Electrical Systems**
WANG Peng
- 040204 **Jacobi Last Multiplier Method for Equations of Motion of Constrained Mechanical Systems**
CHEN Xiang-Wei, MEI Feng-Xiang
- 040205 **Simultaneous Synchronization and Anti-Synchronization of Two Identical New 4D Chaotic Systems**
GUO Rong-Wei
- 040301 **Multipartite Spin Entangled States in Quantum Dots with a Quantum Databus Based on Nano Electro-Mechanical Resonator**
ZHU Zhi-Cheng, TU Tao, GUO Guo-Ping
- 040302 **Photon Distribution of a Squeezed Chaotic State**
FAN Hong-Yi, ZHOU Jun, XU Xue-Xiang, HU Li-Yun
- 040303 **A Three-Node QKD Network Based on a Two-Way QKD System**
HAN Jia-Jia, SUN Shi-Hai, LIANG Lin-Mei
- 040304 **Effect of the Velocity-Dependent Potentials on the Bound State Energy Eigenvalues**
O. Bayrak, A. Soylu, I. Boztosun
- 040305 **High-Capacity Quantum Secure Direct Communication Based on Quantum Hyperdense Coding with Hyperentanglement**
WANG Tie-Jun, LI Tao, DU Fang-Fang, DENG Fu-Guo
- 040401 **Cosmological Dynamics of de Sitter Gravity**
AO Xi-Chen, LI Xin-Zhou, XI Ping
- 040501 **Effects of Time Delay on Stability of an Unstable State in a Bistable System with Correlated Noises**
LI Chun, MEI Dong-Cheng
- 040502 **Weak Signal Frequency Detection Method Based on Generalized Duffing Oscillator**
SHI Si-Hong, YUAN Yong, WANG Hui-Qi, LUO Mao-Kang
- 040503 **Stable Flocking of Multiple Agents Based on Molecular Potential Field and Distributed Receding Horizon Control**
ZHANG Yun-Peng, DUAN Hai-Bin, ZHANG Xiang-Yin
- 040504 **Chaos Control in Random Boolean Networks by Reducing Mean Damage Percolation Rate**
JIANG Nan, CHEN Shi-Jian
- 040505 **Time Evolution of a Harmonic Chain with Fixed Boundary Conditions**
LU Hong, BAO Jing-Dong
- 040701 **Influence of Fabricating Process on Gas Sensing Properties of ZnO Nanofiber-Based Sensors**
XU Lei, WANG Rui, LIU Yong, DONG Liang
- ## THE PHYSICS OF ELEMENTARY PARTICLES AND FIELDS
- 041101 **Peak of Chiral Susceptibility and Chiral Phase Transition in QED₃**
ZHOU Yu-Qing, YANG Yong-Hong

FOR AUTHOR'S USE ONLY
— CHINESE PHYSICS LETTERS

041201 **Associated Production of a Neutral Top-Higgs with Top Quark Pairs at the LHC within the TC2 model**
LI Bing-Zhong, HAN Jin-Zhong

NUCLEAR PHYSICS

042101 **^{174}Hf and ^{174}Yb by the Projected Shell Model with Improved 4-quasiparticle basis**
CHEN Fang-Qi, ZHOU Xian-Rong

ATOMIC AND MOLECULAR PHYSICS

043101 **Lifetime Measurement for $6snp$ Rydberg States of Barium**
SHEN Li, WANG Lei, YANG Hai-Feng, LIU Xiao-Jun, LIU Hong-Ping

043201 **Elastic Scattering between Ultracold ^{23}Na and ^{85}Rb Atoms in the Triplet State**
HU Qiu-Bo, ZHANG Yong-Sheng, SUN Jin-Feng, YU Ke

043301 **Field-Free Molecular Orientation Induced by Nonresonant Square Laser Pulses**
XU Shu-Wu, HUANG Yun-Xia, JI Xian-Ming

043401 **Measurement of Absolute Atomic Collision Cross Section with Helium Using ^{87}Rb Atoms Confined in Magneto-Optic and Magnetic Traps**
WANG Ji-Cheng, ZHOU Ke-Ya, WANG Yue-Yuan, LIAO Qing-Hong, LIU Shu-Tian

043402 **Second Harmonic Generation in Scanning Probe Microscopy for Edge Localization**
HU Xiao-Gen, LI Yu-He, LIN Hao-Shan, WANG Dong-Sheng, QI Xin

FUNDAMENTAL AREAS OF PHENOMENOLOGY(INCLUDING APPLICATIONS)

044201 **Temperature Compensation for Threshold Current and Slope Efficiency of 1.3 μm InAs/GaAs Quantum-Dot Lasers by Facet Coating Design**
XU Peng-Fei, YANG Tao, JI Hai-Ming, CAO Yu-Lian, GU Yong-Xian, WANG Zhan-Guo

044202 **Suppression Impact of Group-Velocity Dispersion on the Cell of Pulse Cleaning**
LI Jing, DENG Ying, WANG Jian-Jun, LI Ming-Zhong, XU Dang-Peng, LIN Hong-Huan, ZHU Na, ZHANG Rui, JING Feng

044203 **Sensitive Detection of Individual Neutral Atoms in a Strong Coupling Cavity QED System**
ZHANG Peng-Fei, ZHANG Yu-Chi, LI Gang, DU Jin-Jin, ZHANG Yan-Feng, GUO Yan-Qiang, WANG Jun-Min, ZHANG Tian-Cai, LI Wei-Dong

044204 **Theoretical Revision and Experimental Comparison of Quantum Yield for Transmission-Mode GaAlAs/GaAs Photocathodes**
SHI Feng, ZHANG Yi-Jun, CHENG Hong-Chang, ZHAO Jing, XIONG Ya-Juan, CHANG Ben-Kang

044205 **A Successive Scans Method of Adjusting Scan-Time for Injection Electroluminescent Display Panels**
OU Peng, YANG Gang, JIANG Quan, WANG Jun, HU Jian-Hua, WU Qi-Peng, LUO Kai-Jun

044206 **Q-Switched Thulium-Doped Domestic Silica Fiber Laser**
HU Hui, DU Ge-Guo, YAN Pei-Guang, ZHAO Jun-Qing, GUO Chun-Yu, RUAN Shuang-Chen

044207 **Coupling Frequency Band of the In-Phase Locked Gain Waveguide Array Lasers**
SHA Peng-Fei, XIN Jian-Guo, FANG Li-Ping, LIU Zheng-Fan, ZHOU Ying, YU Song-Lin, WEN Jian-Guo

044208 **Polarized Spatial Splitting of Four-Wave Mixing Signal in Multi-Level Atomic Systems**
FU Yu-Xin, ZHAO Jin-Yan, SONG Yue, DAI Guo-Xian, HUO Shu-Li, ZHANG Yan-Peng

044209 **Suppression of FM-to-AM Conversion in Broadband Third-Harmonic Generation of Nd:Glass Laser**
CHEN Ying, QIAN Lie-Jia, ZHU He-Yuan, FAN Dian-Yuan

044301 **Hysteretic Nonlinearity of Sub-harmonic Emission from Ultrasound Contrast Agent Microbubbles**
QIU Yuan-Yuan, ZHENG Hai-Rong, ZHANG Dong

044701 **Heat Transfer Analysis for Peristaltic Mechanism in Variable Viscosity Fluid**
T. Hayat, F. M. Abbasi, Awatif A. Hendi

- 044702 **Flow of a Viscoelastic Fluid through a Porous Channel with Expanding or Contracting Walls**
SI Xin-Hui, ZHENG Lian-Cun, ZHANG Xin-Xin, SI Xin-Yi, YANG Jian-Hong
- 044703 **Spectral Characteristics of CN Radical ($B \rightarrow X$) and Its Application in Determination of Rotational and Vibrational Temperatures of Plasma**
PENG Zhi-Min, DING Yan-Jun, ZHAI Xiao-Dong, YANG Qian-Suo, JIANG Zong-Lin
- 044704 **Effective Shear Viscosity of Iron under Shock-Loading Condition**
MA Xiao-Juan, LIU Fu-Sheng, SUN Yan-Yun, ZHANG Ming-Jian, PENG Xiao-Juan, LI Yong-Hong
- PHYSICS OF GASES, PLASMAS, AND ELECTRIC DISCHARGES**
- 045201 **Numerically Reproduction of Spatio-Temporal Evolution of Surface Plasmon Polaritons at Dielectric-Plasma Interface**
CHEN Zhao-Quan, LIU Ming-Hai, ZHOU Qi-Yan, HU Ye-Lin, YANG An, ZHU Long-Ji, HU Xi-Wei
- 045202 **Non Planar Electrostatic Solitary Wave Structures in Negative Ion Degenerate Plasma**
S. Hussain N. Akhtar, Saeed-ur-Rehman
- 045203 **Spatial-Temporal Patterns in a Dielectric Barrier Discharge under Narrow Boundary Conditions in Argon at Atmospheric Pressure**
LI Xue-Chen, JIA Peng-Ying, ZHAO Na
- CONDENSED MATTER: STRUCTURE, MECHANICAL AND THERMAL PROPERTIES**
- 046101 **Pressure-Induced Anomalous Phase Transitions and Colossal Enhancements of Piezoelectricity in Ground-State BaTiO_3**
DUAN Yi-Feng, QIN Li-Xia, SHI Li-Wei, TANG Gang
- 046102 **Monte Carlo Simulation of the Potts Model on a Dodecagonal Quasiperiodic Structure**
WEN Zhang-Bin, HOU Zhi-Lin, FU Xiu-Jun
- 046103 **Improving the Quality of the Deteriorated Regions of Multicrystalline Silicon Ingots during General Solar Cell Processes**
WU Shan-Shan, WANG Lei, YANG De-Ren
- 046201 **Molecule Statistical Thermodynamics Simulation of Nanoindentation of Single Crystal Copper with EAM Potential**
TAN Hao, WANG Hai-Ying, XIA Meng-Fen, KE Fu-Jiu, BAI Yi-Long
- 046202 **Surface Effects on the Postbuckling of Nanowires**
LI Bin, LI Chuan-Xi, WEI Cheng-Long
- 046601 **Effect of the Viscosity of Silicone Oil on the Aggregation Behavior of C:F Clusters on a Silicone Oil Liquid Substrate**
DENG Yan-Hong, YE Chao, YUAN Yuan, LIU Hui-Min, CUI Jin
- CONDENSED MATTER: ELECTRONIC STRUCTURE, ELECTRICAL, MAGNETIC, AND OPTICAL PROPERTIES**
- 047101 **Ideal Strengths and Bonding Properties of PuO_2 under Tension**
WANG Bao-Tian, ZHANG Ping
- 047301 **Rectifying Properties of a Nitrogen/Boron-Doped Capped-Carbon-Nanotube-Based Molecular Junction**
ZHAO Peng, LIU De-Sheng, ZHANG Ying, WANG Pei-Ji, ZHANG Zhong
- 047302 **Electronic Density Decay Lengths of Pb Films from First Principles Calculations**
LI Meng, JIN Hong-Bo, LI Jin-Ming, SUN Qiang, JIA Yu
- 047303 **Deflection Reduction of GaN Wafer Bowing by Coating or Cutting Grooves in the Substrates**
SUN Tao, WANG Ming-Qing, SUN Yong-Jian, WANG Bo-Ping, ZHANG Guo-Yi, TONG Yu-Zhen, DUAN Hui-Ling
- 047304 **Electronic Properties of Bilayer Zigzag Graphene Nanoribbons: First Principles Study**
OUYANG Fang-Ping, CHEN Li-Jian, XIAO Jin, ZHANG Hua
- 047401 **Heat Transport in Graphene Ferromagnet-Insulator-Superconductor Junctions**
LI Xiao-Wei

- 047501 Energy Gap Dependence on Mn Content in a Diluted Magnetic Quantum Dot**
P. Nalini, A. John Peter
- 047801 Spectral Resolution Effects on the Lineshape of Photoreflectance**
MA Li-Li, SHAO Jun, LÜ Xiang, GUO Shao-Ling, LU Wei
- 047802 Multilayer Antireflection Coating for Triple Junction Solar Cells**
ZHAN Feng, WANG Hai-Li, HE Ji-Fang, WANG Juan, HUANG She-Song, NI Hai-Qiao, NIU Zhi-Chuan
- 047803 Improved Hole-Blocking and Electron Injection Using a TPBI Interlayer at the Cathode Interface of OLEDs**
LIAN Jia-Rong, NIU Fang-Fang, LIU Ya-Wei, ZENG Peng-Ju
- 047804 Femtosecond Time-Resolved Resonance-Enhanced CARS of Gaseous Iodine at Room Temperature**
HE Ping, FAN Rong-Wei, XIA Yuan-Qin, YU Xin, YAO Yong, CHEN De-Ying
- 047805 Preparation of Gd₂O₂S:Yb,Ho Phosphor via Thermolysis of Sulfur-Contained (Gd,Yb,Ho)[S₂CN(C₄H₈)₃ Phen Complexes**
ZHONG Hai-Yang, LUO Xi-Xian, MA Lu-Bin, ZHANG Ming, XING Ming-Ming, FU Yao
- CROSS-DISCIPLINARY PHYSICS AND RELATED AREAS OF SCIENCE AND TECHNOLOGY**
- 048101 Stress Control in GaN Grown on 6H-SiC by Metalorganic Chemical Vapor Deposition**
CHEN Yao, JIANG Yang, XU Pei-Qiang, MA Zi-Guang, WANG Xiao-Li, WANG Lu, JIA Hai-Qiang, CHEN Hong
- 048102 Growth of 2 μm Crack-Free GaN on Si(111) Substrates by Metal Organic Chemical Vapor Deposition**
WEI Meng, WANG Xiao-Liang, XIAO Hong-Ling, WANG Cui-Mei, PAN Xu, HOU Qi-Feng, WANG Zhan-Guo
- 048201 A Monte Carlo Simulation of a Monomer Dimer CO-O₂ Catalytic Reaction on the Surface and Subsurface of a Face-centered Cubic Lattice**
K. Iqbal, A. Basit
- 048401 Thermoelectric Properties of Te-Doped Ba_{0.32}Co₄Sb_{12-x}Te_x Prepared at HPHT**
REN Guo-Zhong, LIU Yang, MA Hong-An, SU Tai-Chao, LIN Le-Jing, DENG Le, JIANG Yi-Ping, ZHENG Shi-Zhao, JIA Xiao-Peng
- 048701 Scale-Free Brain Networks Based on the Event-Related Potential during Visual Spatial Attention**
LI Ling, JIN Zhen-Lan
- 048702 DNA Conformational Variations Induced by Stretching 3'5'-Termini Studied by Molecular Dynamics Simulations**
QI Wen-Peng, LEI Xiao-Ling

JUST FOR AUTHORS
— CHINESE PHYSICS LETTERS